

A control chart to monitor the process mean based on inspecting attributes using control limits of the traditional X-bar chart

R. C. Quinino, L. L. Ho, F. R. B. Cruz & L. F. Bessegato

To cite this article: R. C. Quinino, L. L. Ho, F. R. B. Cruz & L. F. Bessegato (2020): A control chart to monitor the process mean based on inspecting attributes using control limits of the traditional X-bar chart, Journal of Statistical Computation and Simulation, DOI: [10.1080/00949655.2020.1741588](https://doi.org/10.1080/00949655.2020.1741588)

To link to this article: <https://doi.org/10.1080/00949655.2020.1741588>



Published online: 27 Mar 2020.



Submit your article to this journal [↗](#)



Article views: 21



View related articles [↗](#)



View Crossmark data [↗](#)



A control chart to monitor the process mean based on inspecting attributes using control limits of the traditional \bar{X} -bar chart

R. C. Quinino ^a, L. L. Ho ^b, F. R. B. Cruz ^a and L. F. Bessegato ^c

^aDepartment of Statistics, Universidade Federal de Minas Gerais, Belo Horizonte, Brazil; ^bDepartment of Production Engineering, University of São Paulo, São Paulo, Brazil; ^cDepartment of Statistics, Universidade Federal de Juiz de Fora, Juiz de Fora, Brazil

ABSTRACT

This paper proposes a new control chart, denoted by \bar{X}^{tn} , for evaluating the stability of a process mean, which is based on attribute inspection. In the \bar{X}^{tn} control chart, the mean of the quality characteristic of interest is controlled by a go-no-go gauge device that generates five categorizations. In equally-spaced times, samples of n items are collected, their categories are determined, and random values are generated according to a truncated normal distribution that corresponds to their categories. With these random values, the averages are estimated and the \bar{X}^{tn} control charts are built. Extensive computational experiments shown that the newly introduced \bar{X}^{tn} control charts perform similarly to the usual \bar{X} control chart in terms of average run length, provided that the sample sizes are raised by approximately three additional sample units. Because the \bar{X}^{tn} control charts use attributes, they can be considered a viable alternative to the traditional \bar{X} control chart.

ARTICLE HISTORY

Received 11 February 2019
Accepted 8 March 2020

KEYWORDS

Quality; \bar{X} control chart; attribute and variable control charts; average run length

1. Introduction

Among the most useful tools for monitoring the quality of the characteristics of interest in a manufacturing process, control charts are built to rapidly detect process shifts and, consequently, minimize the number of defective products, as explained by Montgomery [1]. The \bar{X} charts are the type most commonly used to evaluate the stability of a process mean because of their simplicity, ease of implementation, and satisfactory performance in practice. To implement the \bar{X} control charts, a variable inspection is performed to measure the actual values of x and to calculate \bar{x} . The \bar{X} control charts are still a subject of research even though they have been proposed long ago, in the 1920s, because of their practical use and simplicity. For instance, an economic \bar{X} control chart with warning limits was introduced by Chung [2]. Original schemes to detect changes in the averages of the processes were proposed by Nenes and Panagiotidou [3], Aparisi and de Luna [4], and Liu and Xue [5], Garza-Venegas et al. [6], Haq and Khoo [7], among others. Control methods for the

CONTACT R. C. Quinino  roberto@est.ufmg.br  Department of Statistics, Universidade Federal de Minas Gerais, Belo Horizonte, Brazil



Figure 1. Typical progressive gauges used in industry.

averages in a multivariate context were proposed by Montgomery [1], Kenett et al. [8], Makis [9] and Leoni et al. [10].

However, rather than representing the actual value of x , sometimes, a major concern in an attribute inspection is whether a sample unit is conforming, that is, whether x falls within the warning limits. A passing or nonpassing unit ring gauge to check whether the diameter x of a shaft exceeds a limit is a typical example of attribute inspection [11]. Figure 1 illustrates typical progressive gauges that are able to determine in one run whether a unit is oversized or undersized.

Additionally, Montgomery [1] observes that on a per unit basis, variable-type inspections are more expensive and time-consuming than attribute inspections. On the other hand, although attribute control charts have lower operation costs and times than \bar{X} charts, they have the highest average run lengths (ARLs), and for the small samples sizes, which are common in practice, the under-control ARL is hard to fix to the 200 or 370 limits because of the discrete nature of the corresponding distribution.

In fact, an elucidative example is provided by Montgomery [1], in which an \bar{X} chart is compared to an np chart in the detection of the mean shift of a quality characteristic X that follows a normal distribution, $N(50, 2^2)$. Three-sigma control limits and a sample of size $n_{\bar{x}} = 9$ are used in the \bar{X} control chart. The power of this chart to detect a mean shift of one standard deviation equals 0.50. On the other hand, the sample size for the np chart must be at least $n_{np} = 60$ to detect the same mean shift with the same detection power. That is, the sample sizes for the np charts must be more than 6 times larger than that for the \bar{X} charts, $n_{np}/n_{\bar{x}} > 6.6$; therefore, the choice of monitoring variable averages by means of np charts is not encouraging at all for a practitioner.

Many articles have been published in the literature in which the authors have attempted to solve the above practical issue found on a control chart. For instance, Wu and Jiao [12] proposed an attribute control chart to monitor the mean of a variable in which the run length between two consecutive nonconforming samples is checked, where samples are considered nonconforming if a prespecified number of nonconforming items is found in them. Wu et al. [13] proposed the np_x control chart to monitor a process average by attribute inspection, which employs information from each preceding sample, similar to a Shewhart chart, and for each inspected sample, collects the number of items that fall outside the lower and upper warning interval (LWL and UWL) to determine if a number higher than a specified value (U) is found that signals the process may be out of control

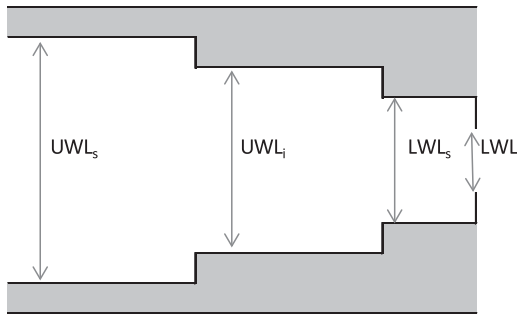


Figure 2. Five category go-no-go gauge.

or, in other words, that the process mean may have suffered a shift in a way that the values LWL, UWL, and U are such that the ARL is set to the minimum. Quinino et al. [14] proposed a new control chart called \bar{X}_{rec} , in which a go-no-go gauge with three categories is used, the number of items in each category is quantified, random numbers from a normal distribution are generated in each one of the three categories, averages are computed, and \bar{X}_{rec} is finally obtained. Quinino et al. [14] reported that the performance obtained in terms of the ARL was significantly better than that of an np_x chart, but the out-of-control ARLs were on average 53% higher than those from a conventional \bar{X} control chart. Ho and Quinino [15] proposed a combination of attribute and variable data to control the variability of a process. However, the papers mentioned earlier do not present ARL values that are similar to those from a traditional \bar{X} control chart. Although possibly economically better, the ARL values are considerably higher than those from the traditional \bar{X} control charts.

In a search for a better performance, Quinino et al. [16] introduced a new control chart, named \bar{X}^{att} chart, in which a go-no-go gauge with five categories (similar to those illustrated in Figure 2) was used to quantify the number of items of the sample that are in each category and to compute \bar{X}^{att} , which is the mean of the mean limits of each category. Quinino et al. [16] determine each category in such a way that the out-of-control ARL is minimized.

The approach proposed by Quinino et al. [16] implies that the distribution of \bar{X}^{att} is discrete, which makes it difficult to fix the in-control ARL at the usual 370 value. To solve this problem, Quinino et al. [16] sought to find the dimensions of the go-no-go gauge in such a way that an ARL of approximately 370 was guaranteed, as usually practiced by companies. Of course, changes on the gauge to comply with the optimal dimensions can cause problems when companies already use standardized metres and do not want to make the changes. Another problem relates to the desire to have formulas of the control limits that are the same as those used in the traditional \bar{X} chart.

In this article, a new proposal of a control chart is presented, called \bar{X}^{tn} , which has a continuous distribution and can be used with the company's usual metre. Consequently, \bar{X}^{tn} generates an in-control ARL exactly equal to 370, as usually practiced in the traditional \bar{X} control chart, and presents control limits with the same formulas as the \bar{X} chart. In practical terms, a sample of size n is collected periodically, and each item is allocated according to the five categories defined by the go-no-go gauge. Then, a measure is generated randomly for each item according to a truncated normal distribution with its upper and lower

limits defined by the dimensions of the go-no-go gauge. With the generated measures, the mean \bar{X}^{tn} is calculated and compared with the LCL and UCL control limits, which can be calculated by the usual formulas of the traditional \bar{X} control chart to decide whether or not the process is under control.

Thus, this newly introduced \bar{X}^{tn} control chart is an alternative to the \bar{X}^{att} control chart when one wants to use the company's attribute meter and ensure a prespecified under-control ARL value. Despite the greater analytical complexity for \bar{X}^{tn} analysis, in operational terms, the control system will not present additional difficulties because of its similarity with the traditional \bar{X} control chart. Furthermore, the same formulas for the control limits of the traditional \bar{X} control chart are used. As shown by extensive computational experiments, the introduced \bar{X}^{tn} control chart has similar out-of-control ARL to the traditional \bar{X} control chart once the sample sizes have approximately three additional units. Because it is simpler and faster to perform measurements by attributes than variable-type inspections, the \bar{X}^{tn} control charts can be competitive in some real situations, as it will be shown shortly.

This article is organized as follows. Section 2 details the sampling distribution of the \bar{X}^{tn} statistic. Section 3 evaluates the performance of the proposed \bar{X}^{tn} control chart compared to the traditional \bar{X} control chart by means of computational simulations and a normal approximation. Section 4 discusses a solution that is not based on the normal approximation. Section 5 illustrates the procedure by a numerical example. Finally, Section 6 presents some conclusions and final remarks.

2. The \bar{X}^{tn} control chart

Motivated by the points presented in the previous section, in the present paper, we seek an attribute control chart without a considerable increase in the sample size that provides in-control and out-of-control ARL values similar to the traditional \bar{X} control chart. It is assumed that a company uses a system that classifies the items into five categories. Figure 2 illustrates some go-no-go gauges considered in this paper.

The quality characteristic X follows a normal distribution. When the process is in control, its mean is known and equal to μ_0 , and when it is out of control, its mean is μ_1 . The variance is known, kept unaltered and denoted by σ^2 . The upper and lower control limits for the standardized values are denoted by UCL and LCL, respectively. The calibrated dimensions of the go-no-go gauge in Figure 2 are denoted as $UWL_S > UWL_i > LWL_S > LWL_i$. One item is of class A if its value of quality characteristic is lower than LWL_i ; of class B if its quality characteristic is in the range $[LWL_i; LWL_S]$; of class C if its quality characteristic is in the range $[LWL_S; UWL_i]$; of class D if its quality characteristic is in the range $[UWL_i; UWL_S]$ and of class E if its quality characteristic is higher than UWL_S . Using a device such as the ones shown in Figure 1, the inspection of each sample of size n can be summarized as $(N_A, N_B, N_C, N_D, N_E)$, being the number of items of class A, B, C, D, E, respectively, with $N_A + N_B + N_C + N_D + N_E = n$. Then, for each inspected item, generate a random value from a truncated normal distribution in which lower and upper truncation points are equal to the limits of the class in which the item was allocated. Let x_{Ar} be the random value taken from a truncated normal $TN(\mu_0, \sigma^2, -\infty, LWL_i)$ distribution related to the r -th item of class A; x_{Bj} , the random value taken from a truncated normal $TN(\mu_0, \sigma^2, LWL_i, LWL_S)$ associated with the j -th item of class B; x_{Ck} , the

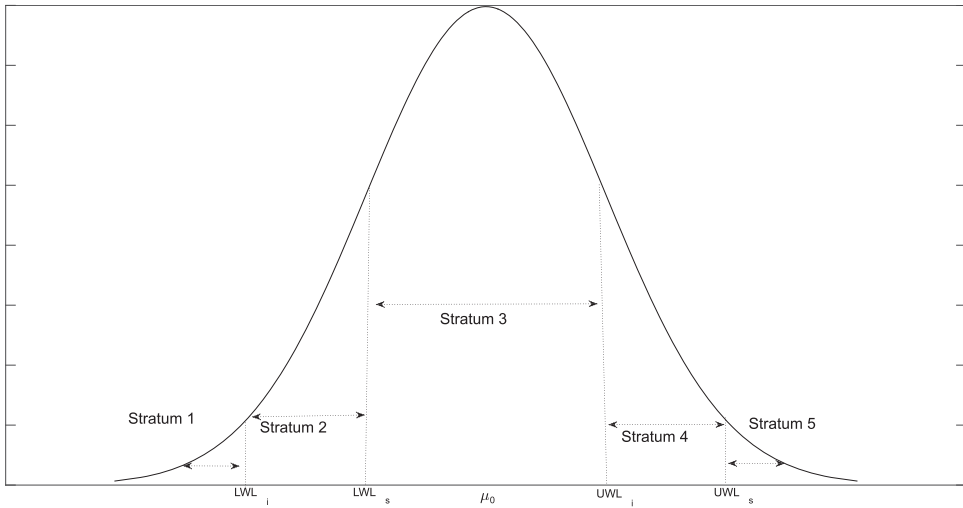


Figure 3. Stratum related to a go-no-go gauge.

random value taken from a truncated normal $TN(\mu_0, \sigma^2, LWL_s, UWS_i)$ for the k -th item of class C; x_{Dz} the random value from a truncated normal $TN(\mu_0, \sigma^2, UWS_i, UWS_s)$ for the z -th item of class D, and finally x_{Es} , the random value from a truncated normal $TN(\mu_0, \sigma^2, UWS_s, \infty)$ for the s -th item of class E. With such information, we compute

$$\bar{X}^{tn} = \frac{X^{tn}}{n} = \frac{\sum_{r=1}^{N_A} x_{Ar} + \sum_{j=1}^{N_B} x_{Bj} + \sum_{k=1}^{N_C} x_{Ck} + \sum_{z=1}^{N_D} x_{Dz} + \sum_{s=1}^{N_E} x_{Es}}{n}$$

and compare it with UCL and LCL to decide if the production process is in control or not. Operationally, we are attaching numerical values to each class through generation of values from truncated normal distributions. In practical terms, the operator or the system will continue employing the same decision rule as that used in the traditional \bar{X} chart.

The assumption is that if the process mean shifts, the values of the random variables N_A, N_B, N_C, N_D, N_E will change, thus signaling the shift and its direction. To find the control limits of the \bar{X}^{tn} chart and to evaluate its performance, the distribution of X^{tn} must be determined. When the process is in control, the procedure in substituting the original measures (but not observed/measured) by the values randomly taken from various truncated normal distributions will yield the same distribution of the original measures X , that is $N(\mu_0, \sigma^2)$. The problem can be viewed as a split of a population into 5 strata (see Figure 3) with re-samplings in each stratum proportional to the probability of each stratum in a normal distribution. This will cause the distribution generated with the resampling of X^{tn} to be equal to the distribution of the quality characteristic $X \sim N(\mu_0, \sigma^2)$.

For a better understanding, Figure 4 illustrates overlapping of two histograms; one originated from the generation of 10 thousand values of a distribution $N(\mu_0 = 0, \sigma^2 = 1)$, and another is the distribution resulting from the generation of normal truncated distributions. As expected, the two distributions can be considered equal.

Thus, the control limits for the \bar{X}^{tn} chart can be obtained analogous to the traditional \bar{X} chart, that is: $UCL = \mu_0 + 3\sigma/\sqrt{n}$ and $LCL = \mu_0 - 3\sigma/\sqrt{n}$ in order to attain in-control

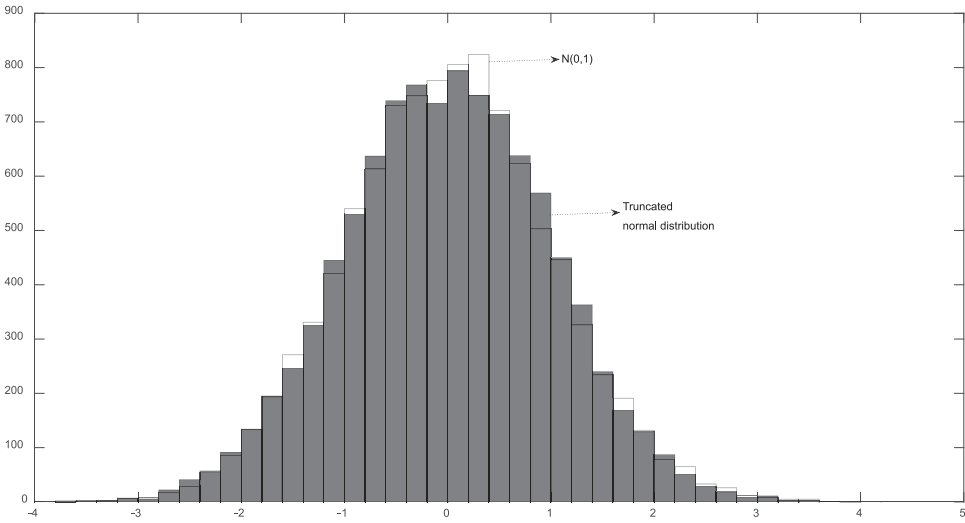


Figure 4. Normal Distribution $N(0,1)$ versus distribution due to the generation of truncated normal distributions.

ARL (ARL_0) of 370. To calculate the out-of-control ARL (ARL_1), the problem is more complicated as X^{tn} does not follow a normal distribution when the process mean shifts from $\mu_0 \rightarrow \mu_1$. Its mean and standard deviation are not respectively equal to μ_1 and σ (but they are for the traditional \bar{X} chart). For example, Figure 5 shows a histogram from a simulation of 10 thousand values of X^{tn} with $UWL_S = 2$, $UWL_i = 1$, $LWL_S = -1$ and $LWL_i = -2$ and $\mu_0 = 0 \rightarrow \mu_1 = 0.8$, that is, when the process is in control, it follows $N(0,1)$ and out-of-control $N(0.8,1)$. From Figure 5, we cannot consider such a distribution as $N(0.8,1)$, as its empirical distribution shape departs from the normal distribution shape, and in addition, its mean is lower than μ_1 but its standard deviation larger than σ . A mathematical discussion about the equality of the distributions of X and X^{tn} is presented in Appendix 1.

Thus, to calculate the distribution of X^{tn} is complicated and yields more difficulty to achieve the exact distribution of \bar{X}^{tn} when the process is out of control. In this sense, one alternative to acquire ARL_1 is to consider the approximation $\bar{X}^{tn} \approx N(\mu^*, \sigma^{*2}/n)$ by the central limit theorem. Note that to get ARL_1 it is considered $\bar{X} \sim N(\mu_1, \frac{\sigma^2}{n})$ in the traditional \bar{X} chart as the quality characteristic X is normally distributed.

The expectation μ^* can be viewed as a weighted average of means of each stratum (as shown in Figure 3),

$$\mu^* = p_A \mu_A^* + p_B \mu_B^* + p_C \mu_C^* + p_D \mu_D^* + p_E \mu_E^* \tag{1}$$

with weights $p_A = P(X < LWL_i)$, $p_B = P(LWL_i < X < LWL_S)$, $p_C = P(LWL_S < X < UWL_i)$, $p_D = P(UWL_i < X < UWL_S)$ and $p_E = P(X > UWL_S)$ obtained adequately with $\mu = \mu_0$ if the process is in control and $\mu = \mu_1$ if the process is out of control. The means μ_i^* , $i = A, B, C, D, E$ are obtained using the truncated normal distribution related to each

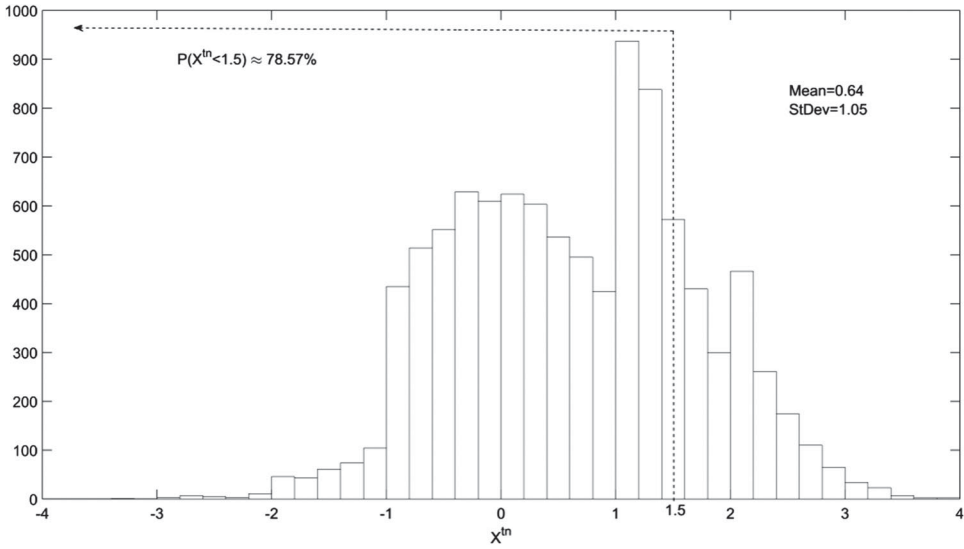


Figure 5. Empirical distribution of X^{tn} when the process is out-of-control.

stratum as:

$$\mu_A^* = \frac{\int_{-\infty}^{LWL_i} xf(x|\mu_0, \sigma^2)dx}{\int_{-\infty}^{LWL_i} f(x|\mu_0, \sigma^2)dx} \tag{2}$$

$$\mu_B^* = \frac{\int_{LWL_i}^{LWL_s} xf(x|\mu_0, \sigma^2)dx}{\int_{LWL_i}^{LWL_s} f(x|\mu_0, \sigma^2)dx} \tag{3}$$

$$\mu_C^* = \frac{\int_{LWL_s}^{UWL_i} xf(x|\mu_0, \sigma^2)dx}{\int_{LWL_s}^{UWL_i} f(x|\mu_0, \sigma^2)dx} \tag{4}$$

$$\mu_D^* = \frac{\int_{UWL_i}^{UWL_s} xf(x|\mu_0, \sigma^2)dx}{\int_{UWL_i}^{UWL_s} f(x|\mu_0, \sigma^2)dx} \tag{5}$$

$$\mu_E^* = \frac{\int_{UWL_s}^{\infty} xf(x|\mu_0, \sigma^2)dx}{\int_{UWL_s}^{\infty} f(x|\mu_0, \sigma^2)dx} \tag{6}$$

$f(x|\mu_0, \sigma^2)$ is the density probability function of a normal distribution. To exemplify, consider the scenario shown in Figure 5; applying (1), we obtain $\mu^* = 0.0026*(-2.3732) + 0.0334*(-1.3832) + 0.5433*0.0000 + 0.3057*1.3832 + 0.1151*2.3732 = 0.6437$, which is closer to the simulation of Figure 5.

It is important to note σ^{*2} can also be viewed as a weighted average of second centred moments related to μ^* of each stratum (as shown in Figure 3):

$$\sigma^{*2} = p_A m_A^* + p_B m_B^* + p_C m_C^* + p_D m_D^* + p_E m_E^* \tag{7}$$

with

$$m_A^* = \frac{\int_{-\infty}^{\text{LWL}_i} (x - \mu^*)^2 f(x|\mu_0, \sigma^2) dx}{\int_{-\infty}^{\text{LWL}_i} f(x|\mu_0, \sigma^2) dx} \quad (8)$$

$$m_B^* = \frac{\int_{\text{LWL}_i}^{\text{LWL}_s} (x - \mu^*)^2 f(x|\mu_0, \sigma^2) dx}{\int_{\text{LWL}_i}^{\text{LWL}_s} f(x|\mu_0, \sigma^2) dx} \quad (9)$$

$$m_C^* = \frac{\int_{\text{LWL}_s}^{\text{UWL}_i} (x - \mu^*)^2 f(x|\mu_0, \sigma^2) dx}{\int_{\text{LWL}_s}^{\text{UWL}_i} f(x|\mu_0, \sigma^2) dx} \quad (10)$$

$$m_D^* = \frac{\int_{\text{UWL}_i}^{\text{UWL}_s} (x - \mu^*)^2 f(x|\mu_0, \sigma^2) dx}{\int_{\text{UWL}_i}^{\text{UWL}_s} f(x|\mu_0, \sigma^2) dx} \quad (11)$$

$$m_E^* = \frac{\int_{\text{UWL}_s}^{\infty} (x - \mu^*)^2 f(x|\mu_0, \sigma^2) dx}{\int_{\text{UWL}_s}^{\infty} f(x|\mu_0, \sigma^2) dx} \quad (12)$$

Using (7) for the scenario depicted in Figure 4, we have $\sigma^* = (0.0026*9.2158 + 0.0334*4.1807 + 0.5433*0.7054 + 0.3057*0.6196 + 0.1151*3.1057)^{0.5} = 1.0455$, which is also coherent with the simulated results of Figure 5.

Applying the expressions (1) and (7), we are able to obtain out-of-control average run lengths using the approximation $\bar{X}^{tn} \approx N(\mu^*, \sigma^{*2}/n)$. Consider $\mu_1 = \mu_0 + \delta\sigma$, which indicates a shift of the process mean signaling an out-of-control condition. This is equivalent to testing the hypotheses: $H_0 : \mu = \mu_0$ versus $H_0 : \mu \neq \mu_0, \mu = \mu_0 + \delta\sigma$. ARL_1 is obtained as $1/(1 - \beta)$, and β is the error of type II expressed as:

$$\begin{aligned} \beta &= P(\text{LCL} < \bar{X}^{tn} < \text{UCL} | \mu = \mu_1 = \mu_0 + \delta\sigma) \\ &= \Phi\left(\frac{\text{UCL} - \mu^*}{\sigma^*/\sqrt{n}}\right) - \Phi\left(\frac{\text{LCL} - \mu^*}{\sigma^*/\sqrt{n}}\right) \end{aligned} \quad (13)$$

$\Phi(\cdot)$ denotes the cumulative normal standard distribution function.

In the next section, the performance of the current proposal is compared with the traditional \bar{X} chart in terms of ARL_1 , fixing ARL_0 equal to 370.

3. Performance of the control charts in monitoring the process mean

The performance of the \bar{X}^{tn} control chart was compared with the \bar{X} chart based on ARL_1 . Sample sizes of units five, six, seven, eight and nine were used in the comparative study because they are values typically used in the traditional \bar{X} control chart. Other sample sizes were also considered, but the results obtained were similar to those obtained for the sample sizes here evaluated. Thus, those results are not included in this paper. The value of $ARL_0 = 370$ was fixed ($\alpha = 0.0027$). Values of ARL_1 were calculated when the in-control mean μ_0 shifted to $\mu_1 = \mu_0 + \delta\sigma$, $\delta = [0.25; 0.5; 1.0; 1.5; 2.0]$. Without loss of generality, we consider the values of the quality characteristic standardized; that is, when the process is in control, we have $N(0, 1)$ and for an out-of-control situation, $N(\delta, 1)$. The values of class limits of the go-no-go gauge were $\text{UWL}_S = 2$, $\text{UWL}_i = 1$, $\text{LWL}_S = -1$ and $\text{LWL}_i = -2$.

Table 1. Values of ARL_1 for the control charts \bar{X} and \bar{X}^{tn} .

N	δ	\bar{X}	\bar{X}^{tn} – normal approximation	\bar{X}^{tn} – simulation
$n = 5$	$ARL_0 (\delta = 0)$	370.40	370.40	370.37
	0.25	133.16	174.22	166.71
	0.5	33.40	51.91	50.01
	1	4.50	7.54	7.43
	1.5	1.57	2.36	2.28
	2	1.08	1.29	1.28
$n = 6$	$ARL_0 (\delta = 0)$	370.40	370.40	370.37
	0.25	115.87	156.95	150.53
	0.5	26.36	42.68	41.20
	1	3.44	5.84	5.75
	1.5	1.33	1.90	1.86
	2	1.03	1.14	1.15
$n = 7$	$ARL_0 (\delta = 0)$	370.40	370.40	370.37
	0.25	101.99	142.40	136.62
	0.5	21.38	35.81	34.72
	1	2.77	4.70	4.65
	1.5	1.20	1.61	1.59
	2	1.01	1.07	1.08
$n = 8$	$ARL_0 (\delta = 0)$	370.40	370.40	370.37
	0.25	90.65	129.98	124.91
	0.5	17.73	30.55	29.74
	1	2.32	3.91	3.87
	1.5	1.12	1.43	1.42
	2	1.00	1.04	1.04
$n = 9$	$ARL_0 (\delta = 0)$	370.40	370.40	370.37
	0.25	81.22	119.28	115.23
	0.5	14.97	26.41	25.79
	1	2.00	3.33	3.30
	1.5	1.07	1.30	1.30
	2	1.00	1.02	1.02
	2.5	1.00	1.00	1.00

Other alternatives are also evaluated, but the conclusions are similar to those described in this paper, so they will not be shown here.

The results are presented in Table 1. The column \bar{X} was obtained through the usual analytical calculations, the column \bar{X}^{tn} – Normal Approximation was obtained according to the approximation $\bar{X}^{tn} \approx N(\mu^*, \sigma^{*2}/n)$, and the column \bar{X}^{tn} – Simulation by the simulation of 800 thousand runs and the lower and upper control limits as 0.135% and 99.865% quantiles. In Appendix 2, a macro that was used to obtain the simulation results is presented, and in Appendix 3, a macro for the normal approximation is described.

We would like to point out the similarity of ARLs from the simulation and normal approximation indicating that such a normal approximation seems reasonable.

As expected, the \bar{X} chart shows a lower ARL_1 than the \bar{X}^{tn} chart for the same sample size. However, if we add three additional sample units to the \bar{X}^{tn} chart, it will yield an ARL_1 lower than or close to the \bar{X} chart. Table 2 shows the ARL_1 results of the \bar{X} chart with typical values $n = 4, 5, 6$ and 7 and the respective ARL_1 values for the \bar{X}^{tn} chart (obtained through simulation) with three additional units. For example, for a shift of $\delta = 1.0$, the \bar{X} control chart with $n = 5$ results in an ARL_1 of 4.5, which is larger than the ARL_1 , of approximately

Table 2. Values of ARL_1 for the control charts \bar{X} and \bar{X}^{tn} .

Chart	\bar{X}	\bar{X}^{tn}	\bar{X}	\bar{X}^{tn}	\bar{X}	\bar{X}^{tn}	\bar{X}	\bar{X}^{tn}
δ / n	4	7	5	8	6	9	7	10
ARL_0	370.40	370.37	370.40	370.37	370.40	370.37	370.40	370.37
0.25	155.22	136.62	133.16	124.91	115.87	115.23	101.99	102.56
0.50	43.89	34.72	33.40	29.74	26.36	25.79	21.38	21.23
1.00	6.30	4.65	4.50	3.87	3.44	3.30	2.77	2.81
1.50	2.00	1.59	1.57	1.42	1.33	1.30	1.20	1.19
2.00	1.19	1.08	1.08	1.04	1.03	1.02	1.01	1.01
2.50	1.02	1.01	1.00	1.00	1.00	1.00	1.00	1.00

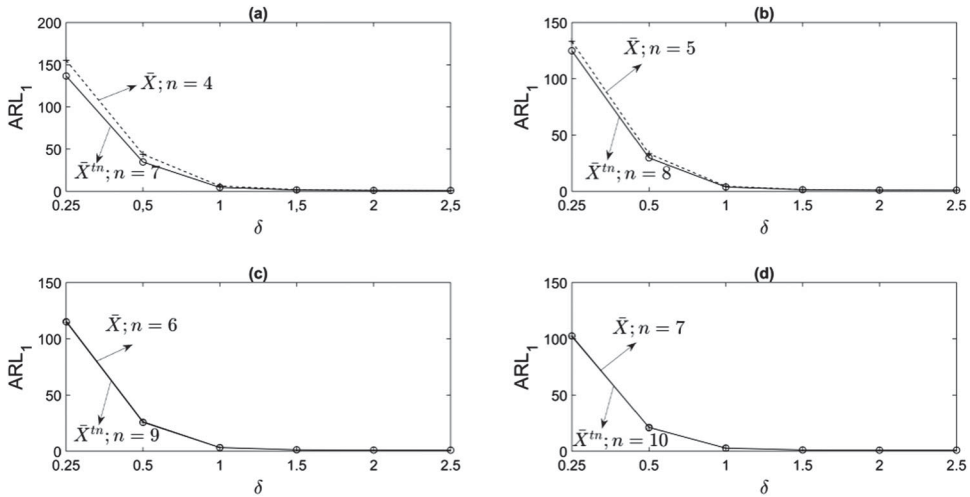


Figure 6. ARL_1 values for the chart \bar{X} compared to ARL_1 values for the chart \bar{X}^{tn} .

3.87 for the \bar{X}^{tn} chart with $n = 8$. For better visualization, we have also included Figure 6, which facilitates the observation of the similarities between the ARL_1 of the \bar{X} chart and the \bar{X}^{tn} chart with 3 additional units. In the case of the inferior part of Figure 6(c,d), the lines visibly overlap, indicating the proximity of the ARL_1 s.

The \bar{X}^{att} chart proposed by Quinino et al. [16] is also included in the comparative study; however, it is not possible to calibrate to achieve equal ARL_0 , as the values of class limits are fixed in the current proposal. While using the go-no-go gauges (utilized by the company) discussed in Sections 3 and 4, the values of ARL_0 that are closer to the target value of 370 for the \bar{X}^{att} control chart are: [215.26, 198.47, 429.95, 400.08 and 232.84] for the respective sample sizes equal to $n = [5, 6, 7, 8 \text{ and } 9]$. The ARL_0 values obtained for the chart \bar{X}^{att} were also used for the \bar{X}^{tn} chart in order to allow for a comparison between both. Table 3 shows the ARL_1 value of \bar{X}^{tn} and \bar{X}^{att} control charts. We can observe that \bar{X}^{att} showed a better performance than the \bar{X}^{tn} control chart. The comparison between these control charts is not simple, as we have different ARL_0 for each sample size. In the specific cases with sample sizes $n = 5$ and 6, the ARL_0 values are similar (215.26 and 198.47, respectively) which leads us to conclude that the ARL_1 of the \bar{X}^{tn} control chart with $n = 6$ is approximately lower than the ARL_1 of the \bar{X}^{att} control chart with $n = 5$.

Table 3. Values of ARL_1 for the control charts \bar{X}^{tn} and \bar{X}^{att} .

n	δ	\bar{X}^{tn} chart	\bar{X}^{att} chart
$n = 5$	$ARL_0 (\delta = 0)$	215.26	215.26
	0.25	104.29	98.49
	0.5	33.85	30.84
	1	5.77	5.26
	1.5	1.99	1.88
	2	1.21	1.18
$n = 6$	$ARL_0 (\delta = 0)$	198.47	198.47
	0.25	87.98	78.88
	0.5	26.75	22.12
	1	4.43	3.62
	1.5	1.64	1.46
	2	1.11	1.07
$n = 7$	$ARL_0 (\delta = 0)$	429.95	429.95
	0.25	154.37	141.03
	0.5	38.49	33.00
	1	4.92	4.21
	1.5	1.63	1.49
	2	1.09	1.06
$n = 8$	$ARL_0 (\delta = 0)$	400.08	400.08
	0.25	133.24	116.16
	0.5	31.27	25.20
	1	3.98	3.24
	1.5	1.43	1.30
	2	1.05	1.03
$n = 9$	$ARL_0 (\delta = 0)$	232.84	232.84
	0.25	78.19	67.90
	0.5	19.21	15.34
	1	2.84	2.34
	1.5	1.24	1.15
	2	1.02	1.01
	2.5	1.00	1.00

The decision between the control charts \bar{X}^{tn} and \bar{X}^{att} for the scenario discussed in this paper needs to consider the reasons that motivated the development of \bar{X}^{tn} control charts. The use of \bar{X}^{att} control chart in an industrial environment in which the dimensions of the go-no-go gauge are fixed may not allow for the use of traditional ARL_0 values, due to the discrete nature of the possible values of the \bar{X}^{att} control chart. In contrast, the \bar{X}^{tn} control chart assumes continuous values, being able to consider any value for ARL_0 and having the advantage of being capable of employing the same control limits of the standard \bar{X} control chart. Moreover, the possible values of ARL_0 for the \bar{X}^{att} control chart are different for each sample size. This may cause some difficulty or disarray in a company that has many products and/or quality characteristics to monitor with different sample sizes. In these cases, the use of standard values of ARL_0 for all cases is very recommendable in order to facilitate the problem identification by the workers. Another aspect that calls for attention in the discrete nature is the possibility of drastic alterations of ARL_0 due to small changes in the control limits. For example, the control limit (LC) for the \bar{X}^{att} control was $LC = 1.2$ for a sample size of $n = 5$, which results in an ARL_0 equal to 215.26. However, small shifts of the control limits, for example $LC = 1.201$, will cause a change of ARL_0 to 454.96. This is

not observed for the \bar{X}^{tn} control chart once it assumes continuous values. These alterations coming from the discretization of \bar{X}^{att} could cause a serious problem, given that in some industrial environments, it is very common to have justified numerical approximations for very small deviations. These small deviations change very little of the ARL_0 value in \bar{X}^{tn} , but they may drastically affect the ARL_0 value of the \bar{X}^{att} control chart. In this sense, we surmise that a quality manager, who considers the previously stated problems as potentially impacting the quality control system, may find the \bar{X}^{tn} chart to be more adequate than the \bar{X}^{att} chart.

In general, evaluations of the items by attributes are cheaper and faster than taking measurements of items; thus it is reasonable to consider the \bar{X}^{tn} chart as a competitive alternative. Consider $c_{\bar{X}^{tn}}$, as the evaluation cost of a single item through a go-no-go gauge (by attributes) and $c_{\bar{X}}$ the evaluation cost of a single item through the use of measurement (by variables). For the economical evaluation, we observe that when the value of ARL_0 is fixed at 370.34, the values of ARL_1 for \bar{X}^{tn} with the size of $(n + 3)$ are lower than or very close to the ARL_1 values for the \bar{X} chart with the size of n . In this sense, the cost of evaluation in a sample of size n by using the \bar{X} chart will be $nc_{\bar{X}}$. For the chart \bar{X}^{tn} , we will use a sample of size $(n + 3)$ in order to have a similar behaviour to the \bar{X} chart in terms of ARL_1 , which results in a cost of $(n + 3)c_{\bar{X}^{tn}}$. Therefore, in economic terms, the chart \bar{X}^{tn} will be preferable to the chart \bar{X} if $(n + 3)c_{\bar{X}^{tn}} < nc_{\bar{X}}$. Hence, the \bar{X}^{tn} control chart will be more economical than the traditional \bar{X} control chart every time that $c_{\bar{X}^{tn}} < \frac{nc_{\bar{X}}}{n+3}$. For a typical situation of \bar{X} control charts with $n = 5$, it would be enough that the costs are such that $c_{\bar{X}^{tn}} < 0.63c_{\bar{X}}$, which is a situation that may occur very often in the industrial environment as stated by Wu et al. [13].

The normal approximation for \bar{X}^{tn} presented in this section shows a reasonable performance mainly for the evaluated cases. However, if the exact distribution of \bar{X}^{tn} (obtained by analytic solution and numerical calculus) were used, the question arises: how is the performance of the proposal affected? In next section, this question will be discussed.

4. Determination of ARL_1 by the analytic approach and numerical calculus

Effectively the determination of $\beta = P(LCL < \bar{X}^{tn} < UCL | \mu = \mu_1 = \mu_0 + \delta\sigma)$ is needed to obtain ARL_1 values as $ARL_1 = 1/(1 - \beta)$. Specifically, we have to determine:

$$\begin{aligned} \beta &= P(LCL < \bar{X}^{tn} < UCL | \mu = \mu_1) \\ &= P\left(LCL < \frac{\sum_{r=1}^{N_A} x_{Ar} + \sum_{j=1}^{N_B} x_{Bj} + \sum_{k=1}^{N_C} x_{Ck} + \sum_{z=1}^{N_D} x_{Dz} + \sum_{s=1}^{N_E} x_{Es}}{n} < UCL | \mu = \mu_1 \right) \end{aligned} \tag{13}$$

The random variables x_A, x_B, x_C, x_D, x_E are truncated normal distributions defined in the beginning of Section 2. The random vector $\mathbf{N} = (N_A, N_B, N_C, N_D, N_E)$ follows a multinomial distribution with parameters $n, p_A, p_B, p_C, p_D, p_E$ (defined also in Section 2) and assumes a finite number of cases, which can be determined by the number of permutations of the sequence $(N_A, N_B, N_C, N_D, N_E)$ constrained to $(N_A + N_B + N_C + N_D + N_E) = n$ and $0 \leq N_i \leq n, i = A, B, C, D, E$. Such a situation is similar to the distribution of n identical balls place in five urns, which can be determined by $k = C_{n+4}^4$. Each urn represents

the 5 classes defined by the limits UWL_S, UWL_i, LWL_S and LWL_i . For example, if $n = 5$, we have 126 possible allocations of \mathbf{N} . Let $W_q, q = 1, \dots, k$ be the representation of each allocation of \mathbf{N} . The probability of each possible configuration of W_q is given by a multinomial distribution with parameters $n, p_A, p_B, p_C, p_D, p_E$. For example, considering the values of the class limits of the go-no-go gauge to be $UWL_S = 2, UWL_i = 1, LWL_S = -1$ and $LWL_i = -2$ and the distribution of the quality characteristic in the out-of-control situation to be given by $X \sim N(\mu_1 = 0.5; \sigma = 1)$, the probability of a particular value for W_q , as in $W_q = (N_A = 1; N_B = 0; N_C = 2; N_D = 2; N_E = 0)$, is calculated by

$$\begin{aligned} P(W_q) &= \frac{n!}{n_A!n_B!n_C!n_D!n_E!} p_A^{n_A} p_B^{n_B} p_C^{n_C} p_D^{n_D} p_E^{n_E} \\ &= \frac{5!}{1!0!2!2!0!} 0.0013^1 \times 0.0214^0 \times 0.4772^2 \times 0.3413^2 \times 0.1587^0 \\ &= 0.0042. \end{aligned}$$

With the use of the variable $W_q, q = 1, \dots, k$, the equation (13) can be written as

$$\begin{aligned} \beta &= \sum_{q=1}^k P(nLCL < \sum_{r=1}^{N_A} x_{Ar} + \sum_{j=1}^{N_B} x_{Bj} + \sum_{k=1}^{N_C} x_{Ck} + \sum_{z=1}^{N_D} x_{Dz} + \sum_{s=1}^{N_E} x_{Es} \\ &< nUCL | \mu_1, W_q) P(W_q) \end{aligned} \tag{14}$$

by the total probability theorem. In the expression (14), the term $P(W_q)$ is relatively easy to calculate. However, the probability at the left hand is quite complicated as it involves a sum of truncated normal distributions. Effectively, the difficulty lies in the multiple integral of the joint density of the truncated normal distribution (whose size is equal to the sample size), subject to the constraint that the sum is less than $nUCL$ and greater than $nLCL$. It is necessary to develop k multiple integrals. For illustrative purposes, consider one term of the expression (14) with $n = 5, (N_A = 1, N_B = 0, N_C = 2, N_D = 2, N_E = 0)$, and the determination of $P(X^{tn} < nUCL)$ is realized through the expression (15) with $X^{tn} = \sum_{r=1}^{N_A} x_{Ar} + \sum_{j=1}^{N_B} x_{Bj} + \sum_{k=1}^{N_C} x_{Ck} + \sum_{z=1}^{N_D} x_{Dz} + \sum_{s=1}^{N_E} x_{Es}$. The computational implementation shows more efficiency if we consider positive and limited regions. Thus, we recommend the usage of the domain R^+ in the probability calculation. For example, $P(X < 1) \approx P(0 < Y < 11)$ with $X \sim N(0; 1)$ and $Y \sim N(10; 1)$. That is, we shift the mean in such a way that the probability of negative values is minimal to occur.

$$\begin{aligned} P(X^{tn} < s = nUCL) &= \int_0^s \int_0^{s-x_{D2}} \int_0^{s-x_{D2}-x_{D1}} \int_0^{s-x_{C2}-x_{D1}-x_{D2}} \int_0^{s-x_{C1}-x_{C2}-x_{D1}-x_{D2}} f(x_{A1}) \\ & f(x_{C1})f(x_{C2})f(x_{D1})f(x_{D2})dx_{A1}dx_{C1}dx_{C2}dx_{D1}dx_{D2} \end{aligned} \tag{15}$$

with

$$\begin{aligned} f(x_{A.}) &= \frac{f(x|\mu_0, \sigma^2)}{\int_{-\infty}^{LWL_i} f(x|\mu_0, \sigma^2)dx} I(X < LWL_i); \\ f(x_{B.}) &= \frac{f(x|\mu_0, \sigma^2)}{\int_{LWL_i}^{LWL_s} f(x|\mu_0, \sigma^2)dx} I(LWL_i < X < LWL_s); \end{aligned}$$

Table 4. Values of ARL_1 for the control charts \bar{X} and \bar{X}^{tn} using the expression (14).

n	δ	\bar{X} chart	\bar{X}^{tn} – normal approximation	\bar{X}^{tn} – simulation	\bar{X}^{tn} – integral
$n = 5$	$ARL_0(\delta = 0)$	370.40	370.40	370.37	370.45
	0.25	133.16	174.22	166.71	166.98
	0.5	33.40	51.91	50.01	49.99
	1	4.50	7.54	7.43	7.42
	1.5	1.57	2.36	2.28	2.28
	2	1.08	1.29	1.28	1.28
$n = 6$	$ARL_0(\delta = 0)$	370.40	370.40	370.37	370.27
	0.25	115.87	156.95	150.53	150.42
	0.5	26.36	42.68	41.20	41.24
	1	3.44	5.84	5.75	5.75
	1.5	1.33	1.90	1.86	1.86
	2	1.03	1.14	1.15	1.15
$n = 7$	$ARL_0(\delta = 0)$	370.40	370.40	370.37	370.46
	0.25	101.99	142.40	136.62	136.68
	0.5	21.38	35.81	34.72	34.72
	1	2.77	4.70	4.65	4.64
	1.5	1.20	1.61	1.59	1.59
	2	1.01	1.07	1.08	1.08
	2.5	1.00	1.00	1.01	1.01

$$f(x_{C.}) = \frac{f(x|\mu_0, \sigma^2)}{\int_{LWL_s}^{UWL_i} f(x|\mu_0, \sigma^2) dx} I(LWL_s < X < UWL_i);$$

$$f(x_{D.}) = \frac{f(x|\mu_0, \sigma^2)}{\int_{UWL_i}^{UWL_s} f(x|\mu_0, \sigma^2) dx} I(UWL_i < X < UWL_s);$$

$$f(x_{E.}) = \frac{f(x|\mu_0, \sigma^2)}{\int_{UWL_s}^{\infty} f(x|\mu_0, \sigma^2) dx} I(X > UWL_s).$$

The complexity increases as the sample size n increases. For example, for a sample size of $n = 7$, there will be seven integrals. The computational implementation was developed in MATLAB using the functions proposed by Hosea M. [17] and Hannak G. [18] that employ MATLAB's own functions in a recursive system for simple, double and triple integrals using the adaptive quadrature algorithm. Table 4 presents the results using expression (14), and the programme is in Appendix 4. From Table 2, we conclude that the three methods provide similar results. However, the last alternative (using expression (14) and the programme described in Appendix 3) is extremely inefficient. Using a computer with an Intel® Core™ i7-7700 CPU and 4.2 GHz processor with 16 GB Ram, approximately 240 hours were spent for each sample size of Table 3. In these terms, we understand that the best alternative is to consider the normal approximation. Note that, if the practitioner intends to exactly employ the proposal of this paper, then Tables 1 and 2 provide reasonable designs without running the macros.

5. Numerical example

A numerical example is presented in this section. The performance of the proposed approach was presented in the previous section. The aim of this section is to present a

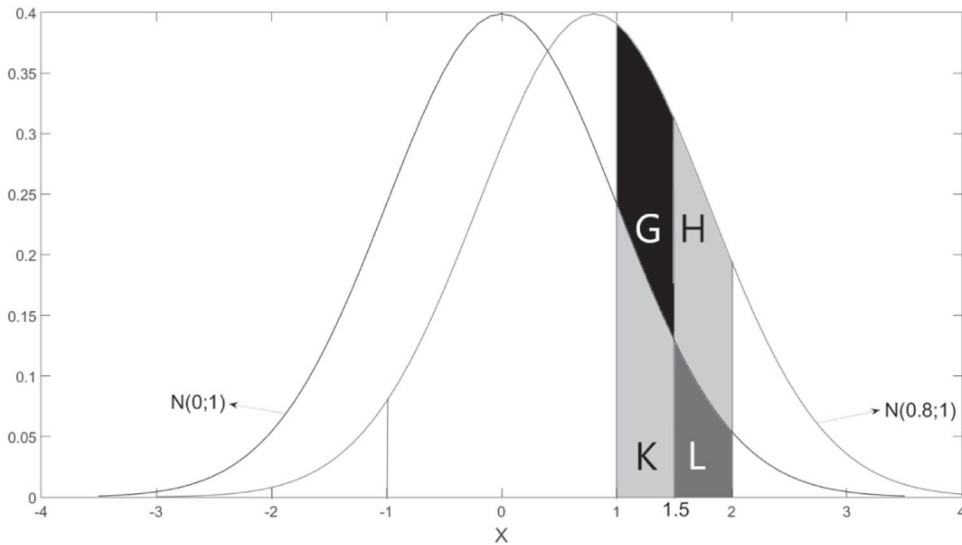


Figure 7. $P(X^{tn} \leq x | \underline{w} < x < \bar{w})$ in the out of control situation.

Table 5. Description of the eight last samples extracted from the production.

Sample	Type A	Type B	Type C	Type D	Type E	\bar{X}^{tn}	Decision (UCL = 103.54; LCL = 96.47)
1	$N_A = 0$	$N_B = 1$	$N_C = 7$	$N_D = 0$	$N_E = 1$	97.98	In control
2	$N_A = 0$	$N_B = 1$	$N_C = 7$	$N_D = 0$	$N_E = 0$	97.57	In control
3	$N_A = 0$	$N_B = 1$	$N_C = 5$	$N_D = 2$	$N_E = 0$	93.32	Out of control
4	$N_A = 0$	$N_B = 0$	$N_C = 7$	$N_D = 1$	$N_E = 0$	98.64	In control
5	$N_A = 0$	$N_B = 1$	$N_C = 5$	$N_D = 2$	$N_E = 0$	97.43	In control
6	$N_A = 1$	$N_B = 1$	$N_C = 1$	$N_D = 5$	$N_E = 0$	99.10	In control
7	$N_A = 1$	$N_B = 0$	$N_C = 5$	$N_D = 2$	$N_E = 0$	96.43	Out of control
8	$N_A = 0$	$N_B = 1$	$N_C = 6$	$N_D = 0$	$N_E = 1$	101.50	In control

practical situation to help a user decide whether to implement the proposed approach. Here, we have adapted an example cited by Montgomery [1] and Quinino et al [14] in which piston rings for automotive engines are produced by a forging process. The objective is to comply with different specifications from the market. We wish to establish control of the inside diameter (D) of the piston rings manufactured by this process. We assume that it is not possible (it is economically costly) to make a direct measurement of the diameter; thus, the attributes are evaluated using the equipment shown in Figure 2.

In this example, the quality engineer decided to use $n = 8$ rings in each sample in order to have a similar ARL_1 of the \bar{X} chart. When the process is in control, the parameters are $\mu_0 = 100.00$ mm and $\sigma_0 = 10.00$ mm. The engineer is concerned with detecting a change within one or more standard deviations. The limits of the classes of the go-no-go gauge device are $UWL_s = 120$ mm, $UWL_i = 110$ mm; $LWL_s = 90$ mm and $LWL_i = 80$ mm. The control limits of the \bar{X}^{tn} chart are exactly the same as those of the \bar{X} chart, that is, $UCL = 100 + 3 \times \frac{10}{\sqrt{8}} = 103.54$ and $LCL = 100 - 3 \times \frac{10}{\sqrt{8}} = 96.47$ for $\alpha = 0.0027$.

Table 5 illustrates the evaluation procedure along the production process for the last eight samples extracted from the production line. For each sample, the number of items in each category is determined, each representative value for each category is calculated and the value \bar{X}^{tn} is determined, as an average for the values generated by the respective truncated normal distribution. If $LCL < \bar{X}^{tn} < UCL$, the process is considered in control. Otherwise, it is considered out of control. Samples 3 and 7 indicate that the process was out of control, while the others indicate otherwise. When the process was considered out of control, some verification and adjustments were necessary (Figure 7).

6. Conclusions

In this paper, a new control chart, called the \bar{X}^{tn} control chart, is proposed for process mean monitoring as an alternative to the \bar{X} control chart when information related to the values of a quality characteristic is only available as attributes. The implementation of the proposed technique is simple and considers control limits that normally are already calculated for the traditional \bar{X} control chart. Therefore, the proposed control chart is easy for the operators to understand and use.

In all cases examined, the \bar{X}^{tn} control chart with three additional units in the samples showed a performance similar to that of the traditional \bar{X} control chart. Therefore, the proposed chart can be viewed as an alternative to be employed when information on the quality characteristic is available only through attribute inspection. In many practical situations, obtaining data through attributes is more economical and operationally easier than taking measurements on a continuous scale.

In this article, the detection of changes in the average of the process was discussed; thus, future works need to discuss the detection of changes in the process variance as well as the joint detection of the mean and variance, such as in Costa and Rahim [19]. Another interesting point would be to use attribute measures to control the coefficient of variation based on, for example, Baocai and Bingxing [20]. Because the \bar{X}^{tn} chart is a Shewhart-type control chart, in future work, a combination of an \bar{X}^{tn} control chart and a CUSUM control chart, or an EWMA control chart (i.e. a CUSUM or EWMA chart using \bar{X}^{tn} as the statistic) may be developed. The overall performance of this scheme must be compared with that of a binomial CUSUM chart or EWMA chart.

Considering that when the process changes from the under-control situation to the out-of-control situation, the \bar{X}^{tn} statistic changes not only the mean but its distribution, the use of the statistic proposed by Zhou et al. [21] can be very efficient in the sense that it used a distribution-free control chart to detect any distributional change. Another possible way to address this problem is through a kernel estimator, as used by Cruz et al. [22].

Finally, another possibility is to explore a multivariate context in the evaluation of the averages by means of attributes. In the present paper, each item is allocated in 5 categories: $[-\infty; LWL_i]$; $[LWL_i; LWL_s]$; $[LWL_s; UWL_i]$; $[UWL_i; UWL_s]$ and $[UWL_s; \infty]$. If we have p variables in an evaluation, we would have to allocate the items in 5^p categories. This could be done by using p go-no-go gauges (one for each quality characteristic). With the results, we could use a truncated multivariate normal distribution in order to generate the information with continuous measurements inside of each one of the 5^p categories. With the generated values, we would be able to find, for example, the Hotelling's T^2 statistics. Therefore, we could compare the performance of the attribute approach and the variable approach. We

believe that the analytical solution would be very complex, making simulation a natural path in a first approach.

Acknowledgement

We would like to thank the editor and two referees for their detailed and insightful comments, which led to a much-improved manuscript.

Disclosure statement

No potential conflict of interest was reported by the author(s).

Funding

This research has been partially funded by the Brazilian agencies CNPq (Conselho Nacional de Desenvolvimento Científico e Tecnológico of the Ministry for Science and Technology), under grants #305515/2018-7 and #301994/2018-8 and FAPEMIG (Fundação de Amparo à Pesquisa do Estado de Minas Gerais), under grant #CEX-PPM-00564-17.

ORCID

R. C. Quinino  <http://orcid.org/0000-0002-2178-1331>

L. L. Ho  <http://orcid.org/0000-0001-9984-8711>

F. R. B. Cruz  <http://orcid.org/0000-0001-5842-5544>

L. F. Bessegato  <http://orcid.org/0000-0002-5004-6790>

References

- [1] Montgomery DC. Introduction to statistical quality control. 6th ed. New York (NY): John Wiley & Sons; 2008.
- [2] Chung KJ. An economic study of X-charts with warning limits. *Comput Ind Eng.* 1993;24(1):1–7.
- [3] Nenes G, Panagiotidou S. An adaptive Bayesian scheme for joint monitoring of process mean and variance. *Comput Oper Res.* 2013;40(11):2801–2815.
- [4] Aparisi F, de Luna MA. Synthetic- \bar{X} control charts optimized for in-control and out-of-control regions. *Comput Oper Res.* 2009;36(12):3204–3214.
- [5] Liu Y, Xue L. The optimization design of EWMA charts for monitoring environmental performance. *Ann Oper Res.* 2015;228(1):113–124.
- [6] Garza-Venegas JA, Tercero-Gómez VG, Ho LL, et al. Effect of autocorrelation estimators on the performance of the \bar{X} control chart. *J Stat Comput Simul.* 2018;88(13):2612–2630.
- [7] Haq A, Khoo BCK. A new synthetic control chart for monitoring process mean using auxiliary information. *J Stat Comput Simul.* 2016;86(15):3068–3092.
- [8] Kenett RS, Zacks S, Ambert D. Modern industrial statistics: with applications in R, MINITAB and JMP. 2nd ed. Chichester: John Wiley & Sons; 2014.
- [9] Makis V. Multivariate Bayesian control chart. *Oper Res.* 2008;56(2):487–496.
- [10] Leoni RC, Costa AFB, Machado MAG. The effect of the autocorrelation on the performance of the T^2 chart. *Eur J Oper Res.* 2015;247(1):155–165.
- [11] Kennedy CW, Hoffman EG, Bond SD. Inspection and gaging. 6th ed. New York (NY): Industrial Press Inc; 1987.
- [12] Wu Z, Jiao J. A control chart for monitoring process mean based on attribute inspection. *Int J Prod Res.* 2008;46(15):4331–4347.
- [13] Wu Z, Khoo MB, Shu L, et al. An np control chart for monitoring the mean of a variable based on an attribute inspection. *Int J Prod Econ.* 2009;121(1):141–147.

- [14] Quinino RC, Ho LL, Trindade ALG. Monitoring the process mean based on attribute inspection when a small sample is available. *J Oper Res Soc.* 2015;66(11):1860–1867.
- [15] Ho LL, Quinino RC. Combining attribute and variable data to monitor process variability: MIX S2 control chart. *Int J Adv Manuf Technol.* 2016;87(9):3389–3396.
- [16] Quinino RC, Bessegato LF, Cruz FRB. An attribute inspection control chart for process mean monitoring. *Int J Adv Manuf Technol.* 2017;90(9):2991–2999.
- [17] Hosea M. *integralN.m.* MATLAB Central File Exchange; 2020. [Retrieved 2020 March 23]. Available from: <https://www.mathworks.com/matlabcentral/fileexchange/47919-integraln-m>.
- [18] Hannak G. *integral_8*, MATLAB Central File Exchange; 2020 [Retrieved 2020 March 23]. Available from: https://www.mathworks.com/matlabcentral/fileexchange/69013-integral_8.
- [19] Costa AFB, Rahim MA. Monitoring process mean and variability with one non-central chi-square chart. *J Appl Stat.* 2004;31(10):1171–1183.
- [20] Baocai G, Bingxing W. Control charts for the coefficient of variation. *Stat Papers.* 2018;59(3):933–955.
- [21] Zhou W, Geng W, Wang Z. Likelihood ratio-based distribution-free sequential change-point detection. *J Stat Comput Simul.* 2014;84(12):2748–2758.
- [22] Cruz FRB, Quinino RC, LL HO. Control charts for traffic intensity monitoring of Markovian multiserver queues. *Qual Reliab Eng Int.* 2019:1–13. In press. <https://doi.org/10.1002/qre.2578>.

Appendix 1. Verification of equality between the control limits for the \bar{X}^{tn} chart and the \bar{X} chart

When the monitoring is made by variables (that is, the measurements are taken), the distribution by a sample of the mean \bar{X} obtained through a random sample of size n extracted from the population $X \sim N(\mu_0; \sigma)$ is well known and expressed by $\bar{X} \sim N\left(\mu_0; \frac{\sigma}{\sqrt{n}}\right)$. Here, X denotes the quality characteristic of interest.

In the case of monitoring by attributes, the item is first classified into one of the classes $[-\infty; LWL_i]$; $[LWL_i; LWL_s]$; $[LWL_s; UWL_i]$; $[UWL_i; UWL_s]$ and $[UWL_s; \infty]$ using a go-no-go gauge device. Then, a random value is generated from a truncated normal distribution in which lower and upper truncation points are equal to the limits of the class in which the item was allocated. The dimensions obtained through this procedure are realizations of a random variable denoted as X^{tn} . Thus, if X^{tn} follows the same distribution of X when the process is in control, then the control limits of \bar{X}^{tn} are the same as the control limits of \bar{X} . That is, if the cumulative distribution $P(X^{tn} \leq x) = P(X \leq x)$, $\forall x$, then X^{tn} and X follow the same distribution and, consequently, the control limits are equal. Let $p_A = P(X < LWL_i)$, $p_B = P(LWL_i < X < LWL_s)$, $p_C = P(LWL_s < X < UWL_i)$, $p_D = P(UWL_i < X < UWL_s)$ and $p_E = P(X > UWL_s)$ be the probabilities of the given classes.

When the process is in control, the probability $P(X^{tn} \leq x)$ can be expressed as $y_1 + y_2 y_3$. The value of y_1 is the sum of probabilities of the classes in which x is larger than its elements; y_2 is the probability of the class that contains x , and y_3 is the conditional probability that the generated random element is lower than x (in the class that contains x). This probability can be expressed as:

$$\begin{aligned}
 P(X^{tn} \leq x | \mu_0) &= \sum_{w \in W} p_w I_{x > \bar{w}} + \sum_{w \in W} p_w I_{\underline{w} < x < \bar{w}} \times \frac{\int_{\underline{w}}^x f(x | \mu_0, \sigma^2) dx}{\int_{\underline{w}}^{\bar{w}} f(x | \mu_0, \sigma^2) dx} \\
 &= \sum_{w \in W} p_w I_{x > \bar{w}} + \sum_{w \in W} I_{\underline{w} < x < \bar{w}} \times \int_{\underline{w}}^x f(x | \mu_0, \sigma^2) dx \\
 &= P(X \leq x | \mu_0)
 \end{aligned} \tag{1}$$

where $W = \{A; B; C; D; E\}$, \underline{w} and \bar{w} denote, respectively, the lower and upper limits of the class w , and $I_{\{\}} is an indicator function.$

Therefore, we can affirm that when the process is in control, the random variables X^{tn} and X follow the same distribution function, and consequently, their sample means \bar{X}^{tn} and \bar{X} also obey the same distribution leading to the same control limits for these two statistics.

When the process is out of control, we have:

$$\begin{aligned}
 P(X^{tn} \leq x|\mu_1) &= \sum_{w \in W} p_w I_{x > \bar{w}} + \sum_{w \in W} p_w I_{w < x < \bar{w}} \times \frac{\int_w^x f(x|\mu_0, \sigma^2) dx}{\int_w^{\bar{w}} f(x|\mu_0, \sigma^2) dx} \\
 &\neq P(X \leq x|\mu_1)
 \end{aligned}
 \tag{2}$$

This difference is because the generation of the random variables under a truncated normal distribution is realized under the same limits of classes used when the process is in control. Therefore, the ratio $\frac{\int_w^x f(x|\mu_0, \sigma^2) dx}{\int_w^{\bar{w}} f(x|\mu_0, \sigma^2) dx}$ in (2) should be $\frac{\int_w^x f(x|\mu_1, \sigma^2) dx}{\int_w^{\bar{w}} f(x|\mu_1, \sigma^2) dx}$. This is a consequence of the loss of information when we do not make the evaluations by variables but by attributes.

For a better understanding, consider a numerical example: when the process is in control $X \sim N(0; 1)$ with $UWL_S = 2$, $UWL_i = 1$, $LWL_S = -1$ and $LWL_i = -2$. In this case, we have:

$$\begin{aligned}
 P(X^{tn} \leq 1.5|\mu_0) &= p_A + p_B + p_C + P(1 < X < 1.5) = 0.0228 + 0.1359 + 0.6827 + 0.0918 \\
 &= 0.9332; \text{ in other words, the results are equal to } P(X \leq 1.5) = 0.9332.
 \end{aligned}$$

Now, consider an out-of-control process, for example $X \sim N(0.8; 1)$; then: $P(X^{tn} \leq 1.5|\mu_1) = p_A + p_B + p_C + P(1 < X < 1.5|\mu_1)P(1 < X < 1.5|\mu_0)/P(1 < X < 1.5|\mu_0)$
 $= 0.0026 + 0.0334 + 0.5433 + 0.2066 = 0.7858$, that is, these results are not equal to $P(X \leq 1.5|\mu_1) = 0.7580$. Figure 5 illustrates this case and contains the value obtained by simulation for $P(X^{tn} \leq 1.5|\mu_1) \approx 0.7857$. Given the class that contains $x = 1.5$, the probability to generate a random value lower than 1.5 might be $(K + G)/(K + G + H + L)$, but the approximate value of $K/(K + L)$ is used, as observed in Figure 7.

Appendix 2. Macro for simulation

```

clear all
tic %
% Detect change in mean (standardized)
u0 = 0; %in control
u1 = 1; % out of control
dp = 1; n = 7; % Sample size
% Dimensions of Standardized Equipment
LWI = u0-2*dp; LWS = u0-1*dp; UWI = u0+1*dp;
UWS = u0+2*dp;
corridas = 500000;
% Distribution under H0
for i = 1:corridas
%Tradicional chart A = random ('normal',u0,dp,n,1);
A1 = mean(A); Saida(i,1) = A1; % chart by Attributes
S1 = sum(A < = LWI); S2 = sum((A > LWI &
A < = LWS));
S3 = sum((A > LWS & A < = UWI));
S4 = sum((A > UWI & A < = UWS));
S5 = sum((A > UWS)); S = [S1 S2 S3 S4 S5];
% Generating Truncated Data
pd = makedist('Normal',u0,dp); r = [];
t = truncate(pd,-inf,LWI); r1 = random(t,S(1,1),1);
r1 = r1'; r = [r r1];
t = truncate(pd,LWI,LWS); r1 = random(t,S(1,2),1);
r1 = r1'; r = [r r1]; t = truncate(pd,LWS,UWI);
r1 = random(t,S(1,3),1); r1 = r1'; r = [r r1];
t = truncate(pd,UWI,UWS); r1 = random(t,S(1,4),1);
r1 = r1'; r = [r r1];
t = truncate(pd,UWS,inf); r1 = random(t,S(1,5),1);
r1 = r1'; r = [r r1];
A2 = mean(r); Saida(i,2) = A2; end
alfa = cdf('normal',-3,0,1);
LI = prctile(Saida(:,1),alfa*100);
LS = prctile(Saida(:,1),(1-alfa)*100);
LIA = prctile(Saida(:,2),alfa*100);
LSA = prctile(Saida(:,2),(1-alfa)*100);
% Distribution under H1
for i = 1:corridas
% Tradicional chart; A = random ('normal',u1,dp,n,1);
A1 = mean(A); Saida(i,3) = A1;
% Distribution under H1
for i = 1:corridas
% Tradicional chart
A = random ('normal',u1,dp,n,1); A1 = mean(A);
Saida(i,3) = A1; % chart by Attributes
S1 = sum(A < = LWI);
S2 = sum((A > LWI & A < = LWS));
S3 = sum((A > LWS & A < = UWI));
S4 = sum((A > UWI & A < = UWS));
S5 = sum((A > UWS)); S = [S1 S2 S3 S4 S5];
% Generating Truncated Data
pd = makedist('Normal',u0,dp); r = [];
t = truncate(pd,-inf,LWI); r1 = random(t,S(1,1),1);
r1 = r1'; r = [r r1];
t = truncate(pd,LWI,LWS); r1 = random(t,S(1,2),1);
r1 = r1'; r = [r r1];
t = truncate(pd,LWS,UWI); r1 = random(t,S(1,3),1);
r1 = r1'; r = [r r1]; t = truncate(pd,UWI,UWS);
r1 = random(t,S(1,4),1); r1 = r1'; r = [r r1];
t = truncate(pd,UWS,inf); r1 = random(t,S(1,5),1);
r1 = r1'; r = [r r1]; A2 = mean(r); Saida(i,4) = A2;
end
% Tradicional chart
ARL0 = 1/(mean((Saida(:,1)
< = LI))+ mean((Saida(:,1) > = LS)))
ARL1 = 1/(mean((Saida(:,3)
< = LI))+ mean((Saida(:,3) > = LS)))
% chart by Attributes
ARL0A = 1/(mean((Saida(:,2)
< = LIA))+ mean((Saida(:,2) > = LSA)))
ARL1A = 1/(mean((Saida(:,4)
< = LIA))+ mean((Saida(:,4) > = LSA)))
toc %

```

Appendix 3. Macro for approximation by central limit theorem

```

clear all
tic %
% Detect change in mean (standardized)
u = 1.5;
u0 = 0;
dp = 1;
n = 7; % Sample size
% Dimensions of Standardized Equipment
LWI = u0-2*dp;
LWS = u0-1*dp;
UWI = u0+1*dp;
UWS = u0+2*dp;

fun = @(x) x.*pdf('normal',x,u0,dp)/
(cdf('normal',LWI,u0,dp));
q1 = integral(fun,-inf,LWI);
p1 = (cdf('normal',LWI,u,dp));
fun = @(x) x.*pdf('normal',x,u0,dp)/
(cdf('normal',LWS,u0,dp)-cdf('normal',LWI,u0,dp));
q2 = integral(fun,LWI,LWS);
p2 = (cdf('normal',LWS,u,1)-cdf('normal',LWI,u,dp));
fun = @(x) x.*pdf('normal',x,u0,dp)/
(cdf('normal',UWI,u0,dp)-cdf('normal',LWS,u0,dp));
q3 = integral(fun,LWS,UWI);
p3 = (cdf('normal',UWI,u,dp)-cdf('normal',LWS,u,dp));
fun = @(x) x.*pdf('normal',x,u0,dp)/
(cdf('normal',UWS,u0,dp)-cdf('normal',UWI,u0,dp));
q4 = integral(fun,UWI,UWS);
p4 = (cdf('normal',UWS,u,dp)-
cdf('normal',UWI,u,dp));
fun = @(x) x.*pdf('normal',x,u0,dp)/
(1-cdf('normal',UWS,u0,dp));
q5 = integral(fun,UWS,inf);

p5 = (1-cdf('normal',UWS,u,dp));
M = q1*p1+q2*p2+q3*p3+q4*p4+q5*p5
fun = @(x) ((x-M).^2).*pdf('normal',x,u0,dp)/
(cdf('normal',LWI,u0,dp));
z1 = integral(fun,-inf,LWI);
fun = @(x) ((x-M).^2).*pdf('normal',x,u0,dp)/
(cdf('normal',LWS,u0,dp)-cdf('normal',LWI,u0,dp));
z2 = integral(fun,LWI,LWS);
fun = @(x) ((x-M).^2).*pdf('normal',x,u0,dp)/
(cdf('normal',UWI,u0,dp)-cdf('normal',LWS,u0,dp));
z3 = integral(fun,LWS,UWI);
fun = @(x) ((x-M).^2).*pdf('normal',x,u0,dp)/
(cdf('normal',UWS,u0,dp)-cdf('normal',UWI,u0,dp));
z4 = integral(fun,UWI,UWS);
fun = @(x) ((x-M).^2).*pdf('normal',x,u0,dp)/
(1-cdf('normal',UWS,u0,dp));
z5 = integral(fun,UWS,inf);
V = z1*p1+z2*p2+z3*p3
+z4*p4+z5*p5;
SV = V^0.5;
V1 = V/n;
SV1 = V1^0.5;

UCL = u0+3*(dp/(n^0.5));
LCL = u0-3*(dp/(n^0.5));
beta = cdf('normal',UCL,M,SV1)-
cdf('normal',LCL,M,SV1);

ARL1 = 1/(1-beta)

```

Appendix 4. Macro for numerical solution

```

clear all
tic
u = 11; %Sob H1
u0 = 10; dp = 1;
n = 5; % Sample size
% Dimensions of Standardized Equipment
pp = cdf('normal',-3,0,1); LS = n*u0+3*((n*dp)^0.5);
L1 = n*u0-3*((n*dp)^0.5); LWI = u0-2*((n*dp)^0.5);
LWS = u0-1*((n*dp)^0.5); UWI = u0+1*((n*dp)^0.5);
UWS = u0+2*((n*dp)^0.5);
p1 = (cdf('normal',LWI,u,1));
p2 = (cdf('normal',LWS,u,1)-cdf('normal',LWI,u,1));
p3 = (cdf('normal',UWI,u,1)-cdf('normal',LWS,u,1));
p4 = (cdf('normal',UWS,u,1)-cdf('normal',UWI,u,1));
p5 = (1-cdf('normal',UWS,u,1)); P = [p1 p2 p3 p4 p5];
i = 1
for x1 = 0:n
for x2 = 0:(n-x1)
for x3 = 0:(n-x1-x2)
for x4 = 0:(n-x1-x2-x3)
x5 = n-x1-x2-x3-x4;
Resultado(i,1) = x1; Resultado(i,2) = x2;
Resultado(i,3) = x3; Resultado(i,4) = x4;
Resultado(i,5) = x5; X = [x1 x2 x3 x4 x5];
Y = mnpdf(X,P); Resultado(i,6) = Y;
z1 = x1; z2 = x2; z3 = x3; z4 = x4; z5 = x5;
L1 = [];
L2 = [];
if z1 > 0
    for x11 = 1:z1
        L1 = [L1;0];    L2 = [L2;LWI];
    end
end
if z2 > 0
for x11 = 1:z2
    L1 = [L1;LWI];    L2 = [L2;LWS];
    end
end
if z3 > 0
for x11 = 1:z3
    L1 = [L1;LWS];    L2 = [L2;UWI];    end
end

if z4 > 0
for x11 = 1:z4
L1 = [L1;UWI];    L2 = [L2;UWS];    end
end

a1 = L2(1); a2 = L1(1); a3 = L2(2); a4 = L1(2);
a5 = L2(3); a6 = L1(3);
a7 = L2(4); a8 = L1(4); a9 = L2(5); a10 = L1(5);
if n = 5
f5 = @(x,y,z,k,v) pdf('normal',x,u,1)/
(cdf('normal',a1,u0,1)- ...
cdf('normal',a2,u0,1))*(x < a1 & x > a2).* ...
pdf('normal',y,u,1)/(cdf('normal',a3,u,1)-
cdf('normal',a4,u0,1)).* ...
(y < a3 & y > a4).* ...
pdf('normal',z,u,1)/(cdf('normal',a5,u,1)-
cdf('normal',a6,u0,1)).* ...
(z < a5 & z > a6).* ...
pdf('normal',k,u,1)/(cdf('normal',a7,u,1)-
cdf('normal',a8,u0,1)).* ...
(k < a7 & k > a8).* ... pdf('normal',v,u,1)/
(cdf('normal',a9,u,1)-cdf('normal',a10,u0,1)).* ...
(v < a9 & v > a10);
upper_y = @(x) (LS-x); upper_z = @(x,y) (LS-x-y);
upper_k = @(x,y,z) (LS-x-y-z); upper_v = @(x,y,z,k)
(LS-x-y-z-k);
q5 = integralN(f5,a2,a1,a4,
upper_y,a6,upper_z, ...
a8,upper_k,a10,upper_v,'AbsTol',1e-3,'RelTol',1e-3);
Resultado(i,7) = 1-q5; upper_y = @(x)(LI-x);
upper_z = @(x,y)(LI-x-y); upper_k = @(x,y,z)(LI-x-y-z);
upper_v = @(x,y,z,k)(LI-x-y-z-k);
q5a = integralN(f5,0,LI,0,upper_y,0,
upper_z,0,upper_k,0,upper_v, ...
'AbsTol',1e-3,'RelTol',1e-3);
Resultado(i,8) = q5a;
i = i+1
end
end
end
end
B1 = Resultado(:,7).*Resultado(:,6);
B2 = Resultado(:,8).*Resultado(:,6);
Beta = B1-B2;
ARL1 = 1/(1-Beta)
Toc

```